Effects of β-α Transformation on the Static and Dynamic Tensile Behavior of Isotactic Polypropylene

JÓZSEF KARGER-KOCSIS[1,*] and JÓZSEF VARGA[2]

[1]Institut für Verbundwerkstoffe GmbH, Universität Kaiserslautern, P.O. Box 3049, D-67653 Kaiserslautern, Germany, and [2]Department of Plastics and Rubber Technology, Technical University of Budapest, H-1521 Budapest, Hungary

SYNOPSIS

It was demonstrated that the mechanical stress-induced $\beta\alpha$-transformation in isotactic polypropylene (iPP) is associated with considerable toughness enhancement. This toughness improvement depends on the test conditions (loading frequency). The toughness of β-iPP was superior to the α-iPP by 13% under static (characterized by a load frequency of ca. 5×10^{-4} Hz) and 70% under dynamic (tensile impact with a loading frequency in the range of ca. $3 \times 10^{2} \cdots 10^{3}$ Hz) conditions, respectively. By applying the essential work of fracture (EWF) concept to single-edge notched tensile (SEN-T) specimens it was shown that for the toughness upgrading observed, energy dissipation in the enlarged plastic zone is responsible. The occurrence of the $\beta\alpha$-transformation was evidenced by differential scanning calorimetry (DSC). Based on DSC measurements it was found that the degree of $\beta\alpha$-transformation depends on the local strain. At high strain values the $\beta\alpha$-conversion is complete (at elogation at break in uniaxial static tensile test), while this transformation is only partial at lower strains (at tensile impact). In addition, in the plastic (or deformation) zone the $\beta\alpha$-conversion changed locally, and can be used for mapping of this region. © 1996 John Wiley & Sons, Inc.

INTRODUCTION

Phase transformation toughening (PTT) is a widely used concept for toughness improvement in metals and ceramics (ref. 1 and references within). PTT is featured by a mechanical stress-induced transformation from a metastable, more dense to a more stable, and less dense crystalline modification, and this transition is associated with a specific volume increase. As a result, the transformation zone at the crack tip becomes subject to compressive stresses, due to which the crack growth is efficiently hindered (crack tip shielding mechanism). This concept became of interest also for polymers. Based on results achieved on isotactic polypropylene (iPP), that underwent β-to-α ($\beta\alpha$) transition during mechanical loading, it was claimed[2,3] that in semi-crystalline polymers PTT is likely to work in the opposite direction. Toughness improvement of β-iPP was attributed to the development of a more perfect crystalline structure, including form (α-form), adapted to the local stress field, and to the formation of an enlarged (stress whitened) plastic zone.[2,3] The $\beta\alpha$-transformation in iPP is linked to a nominal contraction of -2.71% based on the crystallographic densities of the related modifications (0.921 and 0.946 g/cm^3 for the β- and α-iPP, respectively).[4] A number of questions merit further study in connection to the $\beta\alpha$-phase transformation toughened iPP, such as the driving force of this transition and its efficiency as a function of fractional $\beta\alpha$-conversion and mechanical loading frequency.

The aim of the present article is to study the effects of the loading frequency and compare the uniaxial tensile response of α- and β-iPP (i.e., iPP without and with PTT) under static (low freqency) and dynamic (high frequency) conditions, respectively.

* To whom correspondence should be addressed.

Journal of Applied Polymer Science, Vol. 62, 291–300 (1996)
 CCC 0021-8995/96/020291-10

EXPERIMENTALS

β-iPP was produced by incorporating proprietary (Hungarian Patent 209 132) selective β-nucleant (calcium salt of pimelic acid) in 0.1 wt % in a general purpose extrusion molding iPP grade (Tipplen H781F, MFI at 230°C and 21.2 N load: 0.7 dg/min; supplier: Tisza Chemical Works, Hungary). Plates of ca. 1 mm thickness (t) were pressed from this β-nucleated IPP in the following way. iPP in the form of granules (α-iPP) or pellets (β-iPP, previousy melt blended with β-nucleant) were plastified in a screw-driven injection-molding machine without mold and the outcoming melt was deposited on an Al-plate. The latter served as a back plate in the subsequent press cycle. The melt on this Al-plate was transferred quickly in a press the plate of which was kept at 230°C. The PP melt was first pressed within 20 s by using a shape-giving Al-frame of 1 mm thickness, placed on the Al transfer plate. Next, the press was cooled to 115°C, where the melt was isothermally crystallized for 15 min. The press cycle was finished by cooling the press to room temperature (RT) in 6 min. Wide-angle x-ray scattering (WAXS) performed on the specimens by using Ni-filtered CuK_α radiation in a Phillips Micro Müller 111 showed that adding β-nucleant resulted, in fact, in a practically pure β-iPP modification (Fig. 1).

The presence of β-iPP and the occurrence of βα-transformation was demonstrated by differential scanning calorimetry (DSC). DSC scans were registered by a Mettler DSC 30 device at a heating rate of 2°C/min in order to distinguish between the melting of β- ($T_m \approx 150$°C) and α-iPP ($T_m \approx 165$°C), respectively.

Tensile tests were performed at RT under both static and dynamic conditions using the same types of specimens. Dumbbell specimens according to DIN 53448 (A-type) and DIN 53504 (S3A-type), which are later referred to as A and B specimens, were punched from the sheets. Static tensile measurements were run on a Zwick 1445 universal machine (Zwick, Ulm, Germany) at v = 5 mm/min crosshead speed, whereas tensile impact was performed on an instrumented impact pendulum (Ceast, Torino, Italy) at v = 3.7 m/s, set in accordance to DIN 53 448. This pendulum allowed us to monitor and store the fracture history of the specimens, for instance, the load (F) and absorbed energy in function of both time and elongation (x). From these tensile tests the Young's modulus (E-modulus), yield strength (σ_y), necking stress (σ_n), strain at yield, at the onset of necking and at break (ε_y, ε_n, and ε_b) and the total work of fracture (W_f, surface under the F-x curves) were derived.

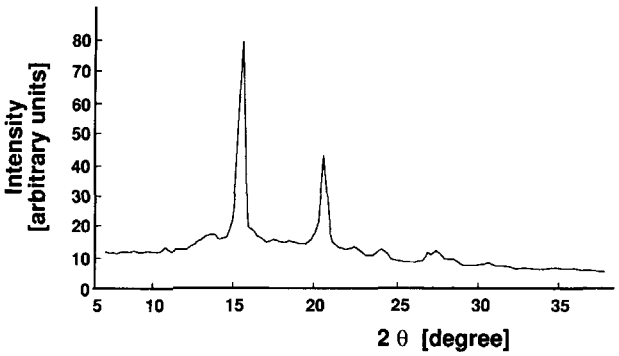

Figure 1 WAXS pattern evidencing the formation of β-iPP due to incorporation of a proprietary β-nucleant in 0.1 wt %.

The heat evolution in the specimens was detected by infrared thermography (IT). IT frames were shot and videotaped *in situ*, for instance, during the loading (v = 5 mm/min) of the specimens. IT analysis was performed by means of a Hughes (Portland, OR) thermal video system. Efforts were focused only on the mapping of the relative temperature rise by choosing an emission factor of 0.9.

In order to determine the toughness as an inherent material parameter the essential work of fracture (EWF) concept (reviewed in refs. 5 and 6) of the ductile fracture mechanics was used. Static tensile loading of single-edge notched specimens (SEN-T; with length and width of 100 and 35 mm, respectively) occurred at the same experimental conditions as for dumbbells. The free ligament (l; cf. Fig. 2) of the SEN-T specimens was varied between 5 and 25 mm. EWF differentiates between the essential (W_e, required to fracture the polymer in its process zone) and nonessential or plastic work (W_p, consumed by various deformation mechanisms in the surrounding plastic zone) for which $W_f = W_e + W_p$ holds (cf. Fig. 2). Taking into consideration that W_e is surface, whereas W_p is volume related, W_f can be given by the related specific work terms (i.e., w_e and w_p, respectively):

$$W_f = w_e l t + \phi w_p l^2 t \tag{1}$$

$$w_f = \frac{W_f}{lt} = w_e + \phi w_p l \tag{2}$$

where ϕ is a shape factor of the plastic zone. Based on eq. (2), the specific essential work of fracture (w_e), being a material parameter, can be easily determined by reading the ordinate intercept of the

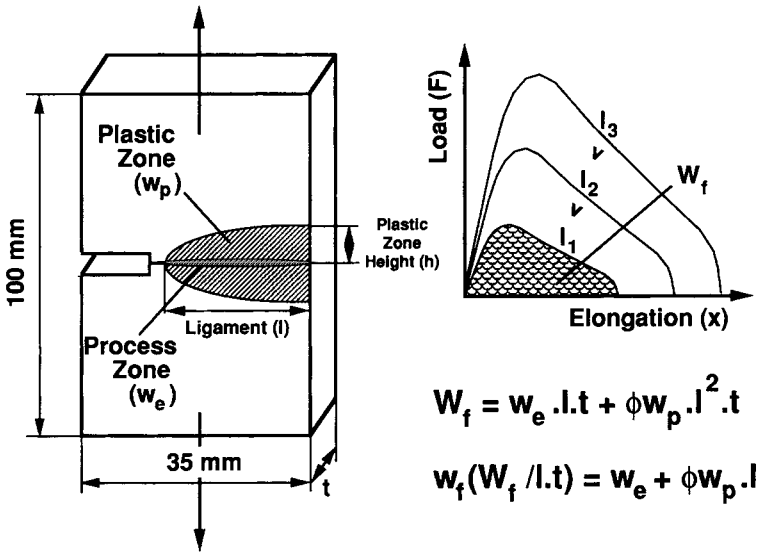

Figure 2 Size of the SEN-T specimens used and determination of the net cross-section related specific work of fracture (w_f) and its constituents (w_e, w_p).

linear plot w_f vs l. The nonessential or plastic work (w_p) can be determined directly from uniaxial tensile tests or indirectly from the slope of the $w_f - l$ regression line by knowing the shape factor ϕ.[7]

Both IT and light microscopic (LM) pictures were taken during loading of the SEN-T specimens.

RESULTS AND DISCUSSIONS

Static Tests

Tensile Behavior

Stress–strain (σ-ε) curves of the α- and β-iPP are compared in Figure 3, and the related tensile characteristics are listed in Table I. One can clearly see that the necking (cold drawing) process is far more marked in α-iPP than in β-iPP. β-iPP, on the other hand, features strong strain hardening so that its ultimate tensile strength (σ_b) supersedes the related value of α-iPP. This is in accordance with previous literature data.[8] The elongation at break (ε_b) is also higher for β-iPP, which is at odds with results of Shi et al.[8] Strain hardening, along with the higher ductility, resulted in improved toughness for β-iPP. Based on the specific work of fracture (w_f) this toughness increment was at about 13%, compared to the α-modification (see Table I).

Fracture Behavior

Figure 4 compares the force–elongation (F-x) curves of SEN-T specimens of the reference α-iPP [Fig. 4(a)] and β-iPP [Fig. 4(b)] at various ligament lengths. One can recognize that the F-x curves in Fig. 4(a) are not fully self-similar, as should be the

Table I Static Tensile Characteristics of α- and β-iPP

Property	Unit	α-iPP	β-iPP
E-modulus	GPa	2.0	1.8
Yield stress (σ_y)	MPa	36.5	29.5
Elongation at yield (ε_y)	%	≈ 12	≈ 7
"Necking" stress (σ_n)	MPa	27.5	—
Elongation at necking (ε_n)	%	≈ 22	—
Ultimate tensile strength (σ_o)	MPa	39.5	44.0
Elongation at break (ε_b)	%	≈ 420	≈ 480
Work of fracture (w_f)	kJ/m^2	≈ 4000	≈ 4520

Testing conditions: RT, v = 1 mm/min, specimen type B.
Designation: —can hardly be defined.

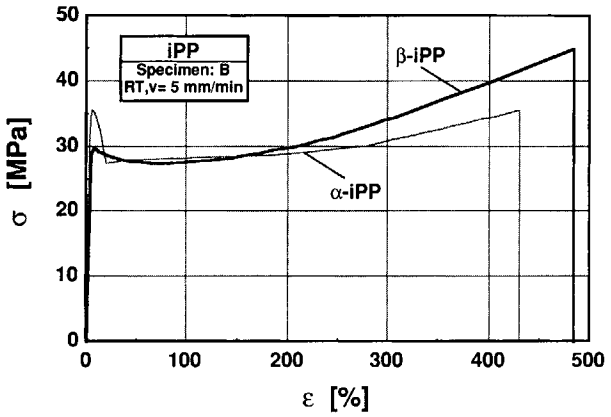

Figure 3 Comparison of the static stress–strain (σ-ε) curves of α- and β-iPP.

case. Deviations in the shape of the F-x curves become more frequent with increasing ligament length. This is due to an incomplete development of the plastic zone: ligament yielding is suppressed by craze-assisted fast fracture at $l \geq 15$ mm. On the contrary, the F-x curves of the β-iPP specimens are identical in form supporting the applicability of the EWF concept. Comparing the F-x curves with the same scale in Figure 4(a) and (b), it is very striking that the β-iPP is more ductile and, thus, more tough than the reference α-iPP. The plastic zone, identified by the stress-whitened region in the SEN-T specimens, shows a very sharp border (due to necking) toward the specimen bulk for α-, whereas hardly any clear border can be observed for β-iPP. In the plastic zone of β-iPP a diffuse yielding process took place (Fig. 5). It has been reported in the literature that the stress-whitened zone in β-iPP is due to the formation of microvoids causing diffuse light scattering.[9,10]

Plotting the total specific work of fracture (w_f) vs. ligament (Fig. 6), the toughness difference between α- and β-iPP becomes obvious. The intercept with the ordinate, for instance, the essential work of fracture (w_e), is the same for both modifications ($\approx$ 34 kJ/m^2). The rationale for this fact can be explained by presuming that w_e depends on the molecular characteristics of the iPP merely. Recall that both α- and β-iPP possess the same molecular parameters because β-iPP is a specially nucleated version of the reference α-iPP. This is in full agreement with our previous results achieved on an other specimen configuration under the same testing conditions.[3] The fact that w_e do not depend on the specimen configuration is lending further support to the validity of the EWF approach.

The basic difference between α- and β-iPP is found in respect to the slope of the regression lines in Figure 6, that is equal with ϕw_p [cf. eq. (2)]. The higher is the slope the higher is the plastic work and, thus, the related energy absorption of the polymer at the same testing conditions. Considering that the ϕw_p term is three to four times higher for β- than for α-iPP suggests a toughness improvement via phase transformation in case of β-iPP. In our previous work $w_p \approx 100$ MJ/m^3 was derived directly from uniaxial tensile tests for both α- and β-iPP.[3] Inserting this value in the related slopes in Figure 6, for β- and α-iPP $\phi \approx 0.20$ and ≈ 0.07 can be computed. These values agree very well again with those established by using deeply double-edge notched tensile (DDEN-T) specimens ($\phi = 0.18$ and $= 0.05$, respectively).[3]

For the development of an elliptical and diamond-shaped plastic zone in DDEN-T specimens

$$\phi = \frac{\pi h}{4l}\,(\text{ellipse}); = \frac{h}{2l}\,(\text{diamond}) \qquad (3)$$

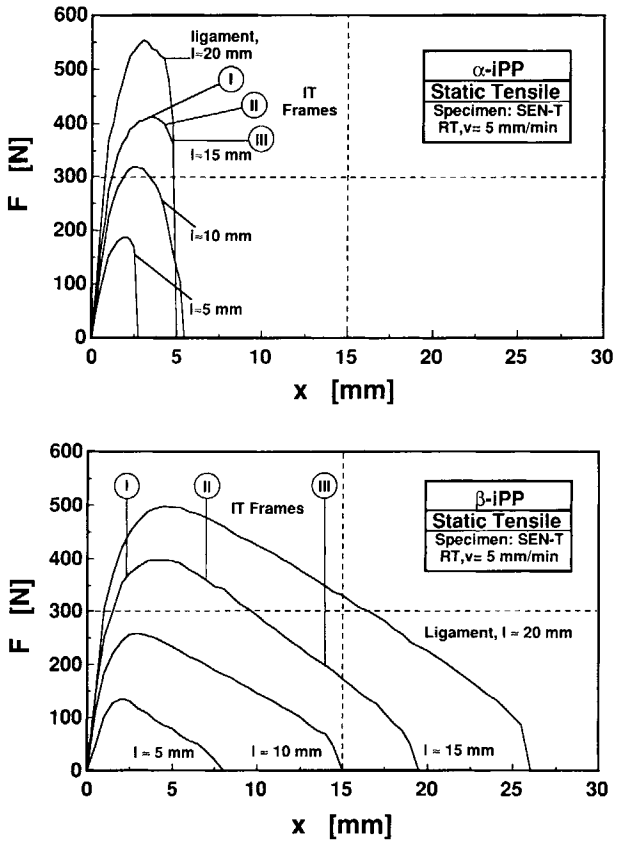

Figure 4 Load–elongation (F-x) curves of the SEN-T specimens at various ligament length (l) for α-iPP (a) and β-iPP (b), respectively. Note: taking position of the IT frames shown in Figure 7 are indicated.

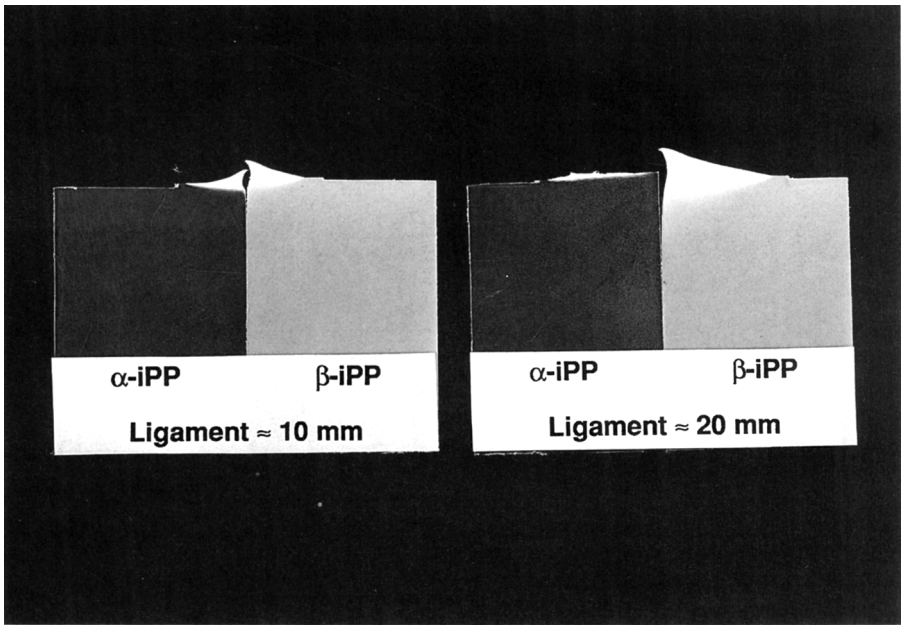

Figure 5 Broken SEN-T specimens of the α- and β-iPP at the same ligament length values (l ≈ 5 and ≈ 20 mm, respectively) showing the difference in the related process zones.

hold, where h is the height of the whole plastic zone.[6,7] Equation 3 seems to work for our SEN-T specimens, if h is defined as the half of the overall plastic zone (or the height of the plastic zone on the half SEN-T specimen) just before final fracture. This approach for definition of "h" in SEN-T specimens is illustrated in Figure 2. Making use of this approch and recovering the height of the plastic zone from the LM and IT pictures taken during loading, ϕ values very similar to the aforementioned ones were derived.

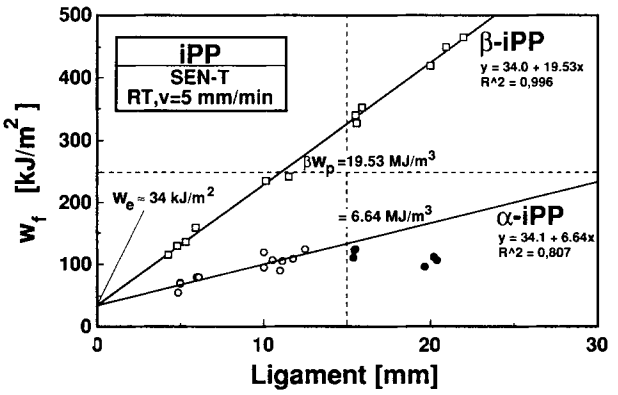

Figure 6 Specific total work of fracture vs. ligament (w_f vs. l) plots for the SEN-T specimens of α- and β-iPP, respectively. Note: data related to fast fracture of α-iPP at l ≥ 15 mm (cf. filled circles), are excluded.

Failure Behavior

Serial IT frames taken from the SEN-T specimens of α- [cf. Fig. 4(a)] and β-iPP [cf. Fig. 4(b)] clearly demonstrate the substantial difference in the shape of the related plastic zones (Fig. 7). The advancing plastic zone is triangle shaped (forming a half diamond prior to fracture) in α-iPP [Fig. 7(a)]. In addition, this IT series hints at the presence of a rather sharp crack. The temperature rise observed along the flanks of the propagating crack is of ca. 5°C [cf. cursor marked points in the thermal map of Fig. 7(a)]. This is direct evidence for the onset of localized yielding, as was shown and discussed in connection to Figure 5. On the contrary, β-iPP fails by crack tip blunting [Fig. 7(b)] associated with the appearance of an enlarged plastic zone. Though the maximum temperature registered is comparable with that of the α-iPP, the hottest spots are located along the free ligament [see the cursor points in the IT frames in Fig. 7(b)]. The overall shape of the plastic zone in β-iPP prior to specimen separation can be approached by a half ellipse. Plotting the height of the plastic zone (as defined above) that was read from the videotaped IT failure sequence in function of the ligament, and accepting a diamond-like and elliptical shape for the plastic zone for α- and β-iPP, respectively, $\phi \approx 0.20$ and ≈ 0.06 were computed. These data are well matched with those

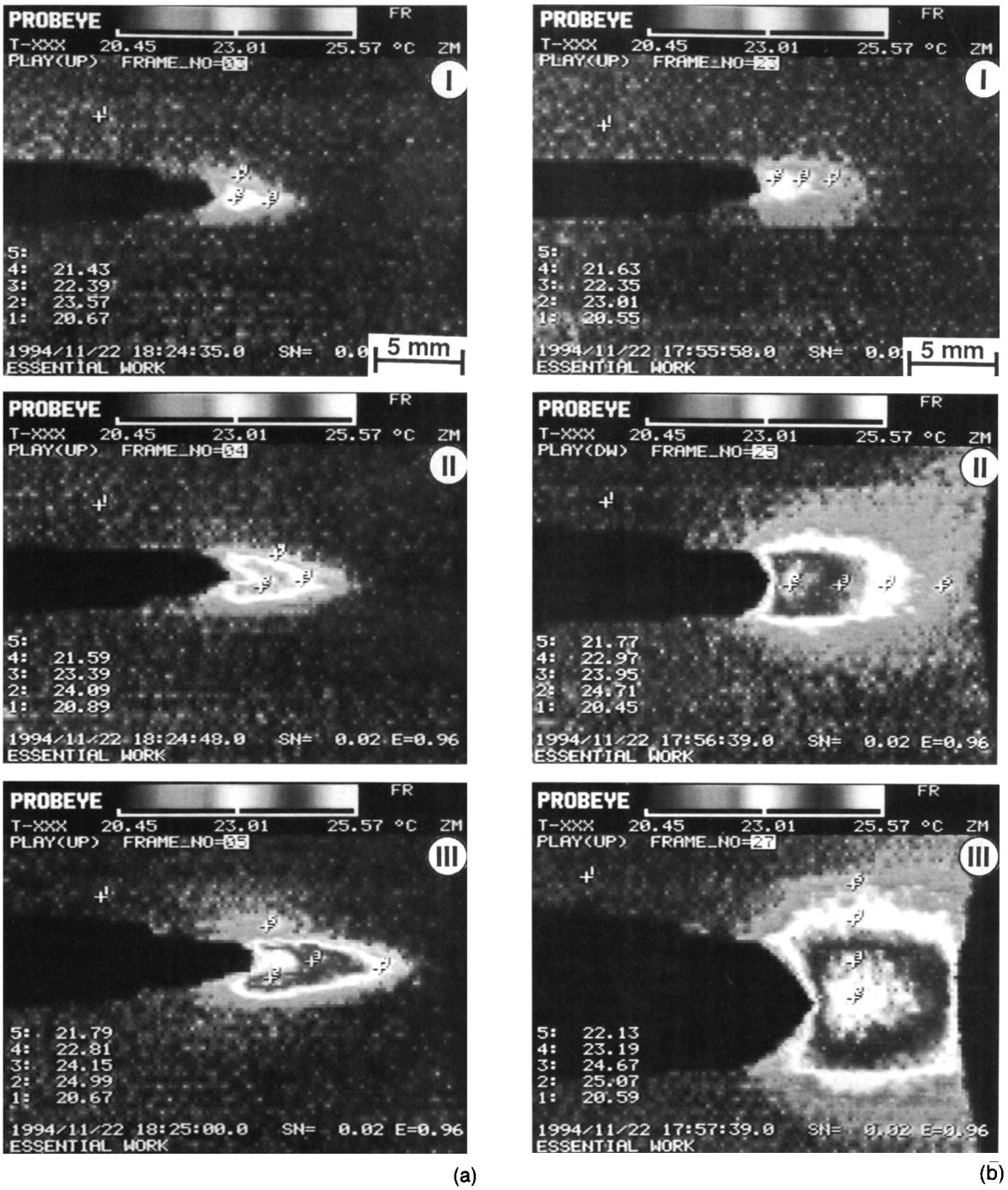

Figure 7 Comparison of serial IT frames taken during the loading of SEN-T specimens of α- (a) and β-iPP (b). Note: the taking position of the thermovision pictures are indicated in Figure 4(a) and 4(b), respectively.

obtained from the slopes by inserting the w_p value originated from separate tensile tests on dumbbell specimens. So, the approach proposed for the determination in SEN-T specimens seems to work well.

Dynamic Tests

Tensile Impact Behavior

σ-ε curves, monitored during tensile impact and showing the energy absorption, as well, are depicted

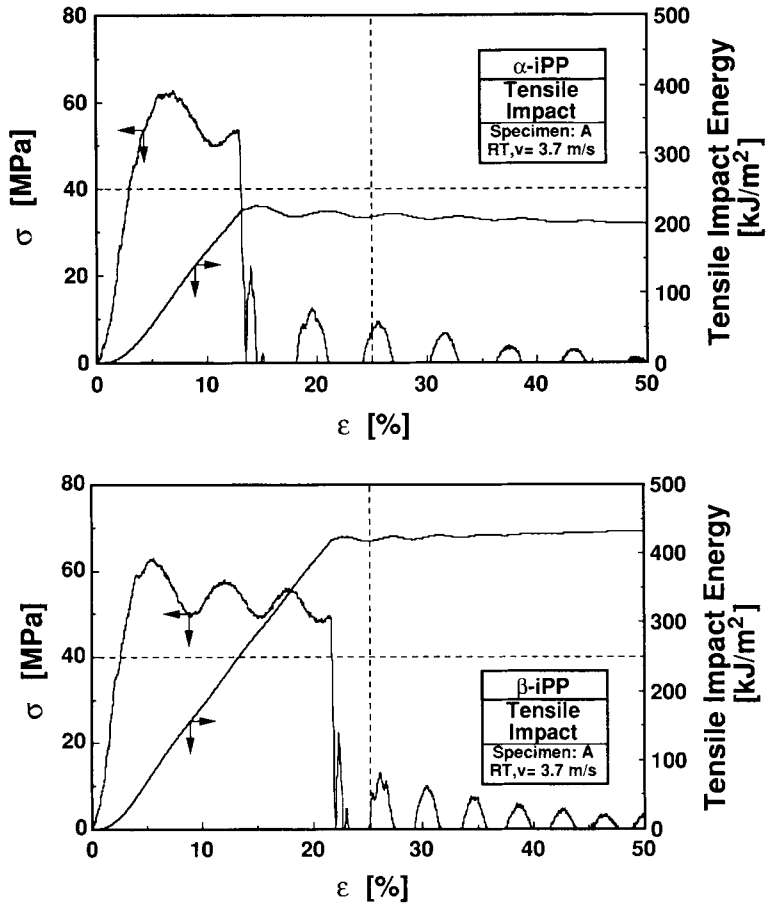

Figure 8 Stress and absorbed energy vs. strain curves due to tensile impact for α-iPP (a) and β-iPP (b) by using the same type of specimen (A).

in Figure 8(a) and 8(b) for α- and β-iPP, respectively. The related tensile characteristics are summarized in Table II. The basic difference in the tensile impact response between α- and β-iPP is that the latter fails at a considerably higher strain. This is associated with an almost doubling of the energy absorption.

Failure Behavior

A peculiar feature of the tensile impact fractograms of β-iPP is the stress (load) oscillation. This oscillation phenomenon was observed, especially in case of polyethylene-terephthalate (PET), a long time ago (refs. 11 and 12, and references within). Its ap-

Table II Dynamic Tensile Characteristics of α- and β-iPP

Property	Unit	α-iPP	β-iPP
E-modulus	GPa	2.5	2.4
σ_y	MPa	63	65
ε_y	%	≈ 7	≈ 6.5
σ_n	MPa	55	52–59[a]
ε_n	%	≈ 11	≈ 10
σ_b	MPa	59	51.5
ε_b	%	≈ 14	≈ 21
Tensile impact strength (w_f)	kJ/m²	≈ 230	≈ 390

Testing conditions: RT, v = 3.7 m/s, specimen type A.
Designation: [a] —lower and upper oscillation thresholds.

pearance was reasoned either by thermal dissipation of the deformation energy[11] or by the presence of a critical stress.[12] IT frames taken just after the breakage of the A-type specimens of α- and β-iPP, respectively, demonstrate very clearly that both the temperature rise and the heated-up field are markedly higher in the β- than in the α-iPP (Fig. 9). This reflects the higher ductility, and thus improved toughness of the β-iPP. Features of the temperature map in Figure 9(b) may be connected to the load oscillations observed. The number of load oscillations observed (i.e., 3) in β-iPP corresponds to the number of temperature fronts that can be well distinguished from one another in Figure 9(b). This hypothesis needs, however, further experimental evidence. Nevertheless, the above finding is likely to corroborate the validity of the thermal fluctuation model of Adrianova et al.[11]

Comparing the tensile characteristics under static (Table I) and dynamic conditions (Table II), it turns out that both stiffness (E-modulus) and strength values are enhanced, while strain parameters are reduced due to an increase in the test frequency. These changes are in full concert with the expectations. Based on the reciprocal value of the time needed to the final fracture of the specimens the freqency range of the static and dynamic tests can be given by ca. $(5\text{–}6) \times 10^{-4}$ Hz and $(1\text{–}30) \times 10^{3}$ Hz, respectively (the scatter is caused by the iPP modifications). As far as toughness is concerned, β-iPP is superior to the α-iPP by 13 and 70% under static and dynamic test conditions, respectively (cf. Tables I and II). This demonstrates that the net effect of $\beta\alpha$-transformation toughening is strongly dependent on the testing conditions, the relative toughness improvement is higher the higher the test frequency is.

Phase Transformation

Although the above several findings were related and explained by a probable $\beta\alpha$-transformation, its occurrence was not yet proven. In order to prove this $\beta\alpha$-transformation, DSC traces were taken from different positions of the specimens that failed under static and dynamic loading, respectively.

Static Tests

Figure 10 depicts the normalized (to the same sample weight) DSC heating traces for samples taken from the plastic zone and specimen bulk, respectively, of an SEN-T specimen of β-iPP. One sample was taken from the fracture surface (DSC trace a), whereas another from the diffuse region ending the plastic zone toward the bulk (DSC trace b). The DSC trace (a) in Figure 10 demonstrates that in the process zone (i.e., fracture surface) the $\beta\alpha$-transformation was completed (conversion is 100%), because the DSC trace is identical with that of the α-iPP. This explains why the same esential work value was found for both α- and β-iPP modifications (cf. Fig. 6). DSC curves of samples taken from the plastic zone [Fig. 10;(b)] and specimen bulk [Fig. 10;(c)], on the other hand, demonstrate how complex the melting of β-iPP is (partial melting of the

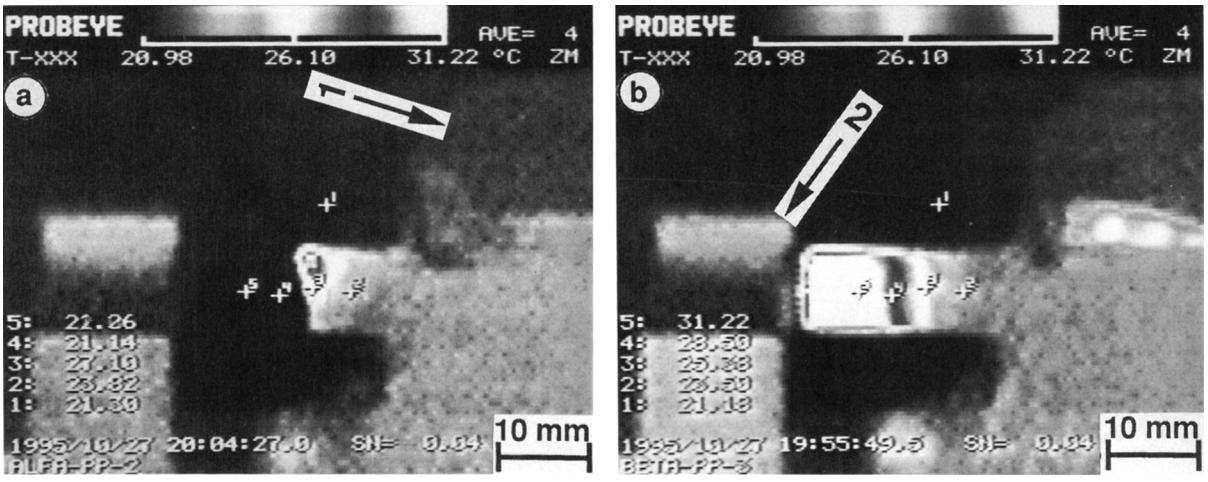

Figure 9 IT frames taken from the tensile impact specimen of α-iPP (a) and β-iPP (b) just after fracture. Notes: the related fractograms are portrayed in Figure 8(a) and 8(b), respectively; arrows indicate for the specimen holding screw (1) and supporting anvil (2) in between the specimen is located.

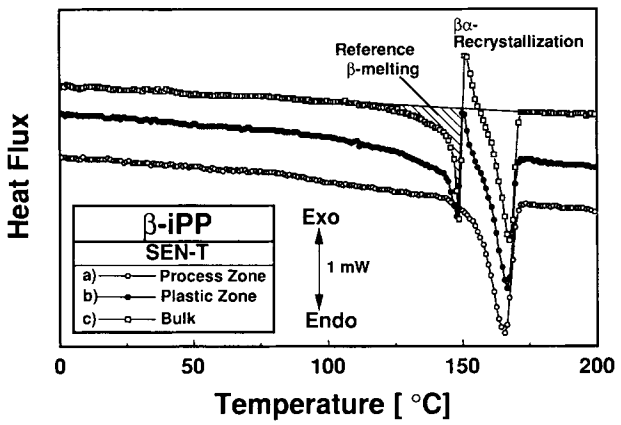

Figure 10 DSC heating traces (registered at 2°C/min) taken from different positions of a SEN-T specimen of β-iPP after static loading. Notes: the DSC traces are normalized to the same sample weight and shifted parallel to one another by 0.5 and 1 mW, respectively.

β-phase, βα-recrystallization and melting of the recrystallized α-phase, being superimposed on one another).[13,14] Comparing the DSC curves (b) and (c) in Figure 10, one can notice that in the plastic zone the βα-transition occurred only partially. Furthermore, it was found that the βα-conversion changes locally within the plastic zone. This feature can well be used for "mapping" of the plastic zone.

The fractional βα-conversion can be estimated (supposing identical DSC testing conditions, incl. sample weight) either by the relative ratio of the melting peak of the β-iPP or α-iPP. For reference purposes, the related β- or α-melting peak of the bulk β-iPP sample can be considered. By this technique it was found that in the border between the plastic zone and specimen bulk the βα-conversion was about 40%. Considering the fact that in the process zone this conversion was 100%, the above finding means that the grade of the βα-transformation changes with the local strain within the plastic zone. DSC traces taken on samples from fully elongated B-type β-iPP specimens did not reveal the presence of any β-modification; here, only α-iPP could be detected. The above findings are in harmony with reports of Varga,[13,14] who studied the features of βα-transformation in β-iPP as a function of specimen strain. He concluded that there was a gradual increase of the βα-conversion as a function of the overall strain.

Dynamic Tests

DSC samples were taken from different positions of the broken half of the β-iPP specimen, the thermal mapping of the fracture surface of which is given in Figure 9(b). Here, one sample was taken again from the fracture surface (DSC trace a; process zone), and the other from the border of the heated up region [cf. Fig. 9;(b)]. The related weight-normalized DSC curves are depicted in Figure 11. This figure shows that even in the fracture surface the βα-transformation was not completed. Based on the aforementioned estimation procedure, here the βα-conversion was of about 25–30%, whereas in the far-field region of ca. 20%. Irrespective of this moderate fractional conversion, a relative high toughness improvement was detected (70%, cf. Table II). Further investigations are necessary, however, to check in to what extent the grade of the βα-transformation affects the toughness, and whether or not it can be influenced by the thermal history of manufacturing of the β-iPP.

CONCLUSIONS

The results of this study performed on the static and dynamic tensile response of isotactic polypropylene (iPP) in its α- and β-form, respectively, can be summarized as follows:

1. the βα-transformation, accompanied with volume contraction in respect to the related crystallographic densities, results in toughness improvement. The direction of this βα-transformation (i.e., contraction) is just the opposite to that of the phase-transformation toughening (PTT) practiced for metals and ceramics. For the latter materials, the tough-

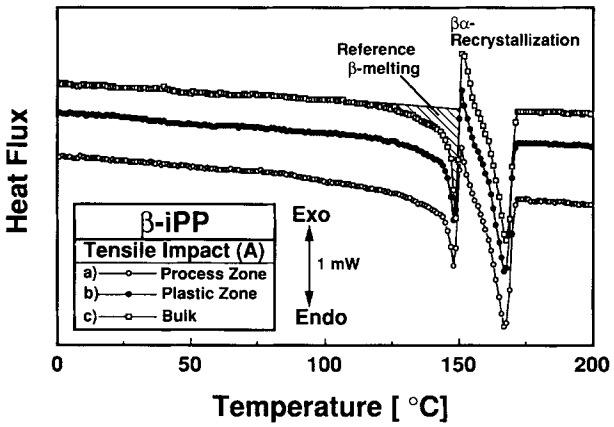

Figure 11 DSC heating traces taken from different positions of an A-specimen of β-iPP after tensile impact [cf. Fig. 9(b)]

ness increasing crack tip shielding mechanism is achieved by volume dilation.

2. The toughness increasing effect of the mechanical stress-induced $\beta\alpha$-transformation is strongly dependent on the testing conditions, more exactly, on the related loading frequency. With increasing frequency (from static toward tensile impact) the relative toughness improvement (compared to the α-iPP, as reference material) was enhanced, as well.
3. The $\beta\alpha$-transformation itself is depending on the local strain field, as demonstrated by DSC traces taken from different sites of the plastic (or deformation) zones in broken specimens. With increasing test frequency the fractional $\beta\alpha$-conversion was reduced.

This work was supported by the German Science Foundation (DFG; Phasenumwandlung, Ka 1202/2-1) and the Hungarian Science and Research Council (OTKA).

REFERENCES

1. R. W. Hertzberg, in *Deformation and Fracture Mechanics of Engineering Materials,* 3rd ed., Wiley, New York, 1989, pp. 353–419.
2. J. Karger-Kocsis, *Polym. Bull.,* **36,** 119 (1996).
3. J. Karger-Kocsis, *Polym. Eng. Sci.,* **36,** 203 (1996).
4. S. Z. D.Cheng, J. J. Janimak, and J. Rodriguez, in *Polypropylene, Structure, Blends and Composites*, J. Karger-Kocsis, Ed., Chapman and Hall, London, 1995, pp.31–55.
5. G. Levita, L. Parisi, and A. Marchetti, *J. Mater. Sci.,* **29,** 4545 (1994).
6. A. G. Atkinson and Y.-W. Mai, *Elastic and Plastic Fracture,* Ellis Horwood, Chichester, 1988.
7. Testing protocol for the essential work of fracture, ESIS TC-4 group, 1993.
8. G. Shi, F. Chu, G. Zhou, and Z. Han, *Makromol. Chem.,* **190,** 907 (1989).
9. T. Yoshida, Y. Fujiwara, and T. Asano, *Polymer,* **24,** 925 (1983).
10. F. Chu, T. Yamaoka, H. Ide, and Y. Kimura, *Polymer,* **35,** 3442 (1994).
11. G. P. Adrianova, A. S. Kecheklyan, and V. A. Kargin, *J. Polym. Sci. A-2,* **9,** 1919 (1971).
12. T. Pakula and E. W. Fischer, *J. Polym. Sci. Phys.,* **19,** 1705 (1981).
13. J. Varga, *J. Thermal. Anal.,* **35,** 1891 (1989).
14. J. Varga, in *Polypropylene, Structure, Blends and Composites*, J. Karger-Kocsis, Ed., Chapman and Hall, London, 1995, pp. 56–115.

Received January 5, 1996
Accepted March 13, 1996